Int. J. Heat Mass Transfer. Vol. 36, No. 6, pp. 1471-1476, 1993
Printed in Great Britain

0017-9310/93 $6.00+0.00

Linear stability of natural convection in a tall vertical slot with a moving sidewall

J.-C. CHEN and C.-K. HSIEH
Department of Mechanical Engineering, National Central University, Chung-Li, Taiwan, R.O.C.

(*Received* 27 *April* 1992 *and in final form* 6 *August* 1992)

Abstract—The effect of a shear force on the stability of natural convection in a tall vertical slot has been studied utilizing linear theory. Our results show that the stability of natural convection is significantly affected by the motion of the sidewall and that sidewall motion creates three types of instability. At small Prandtl numbers, the shear instability is dominant. At higher Prandtl numbers, the flow becomes unstable, creating a buoyant instability induced by the boundary layer near the fixed (unmoving) sidewall. When the sidewall moves slightly downward, the buoyant instability induced by the boundary layer near that moving wall occurs for Prandtl numbers near 10. The critical Prandtl number which marks the transition between the shear and buoyant modes is strongly dependent on the direction and speed of the sidewall movement.

1. INTRODUCTION

CONVECTION stability in a vertical slot with differentially heated sidewalls has been studied by several authors [1–4]. The results showed that the stability limit is a function of the Grashof and Prandtl numbers. For a small Prandtl number fluid ($Pr < 12.7$), the parallel flow undergoes a transition to a stationary multicell flow pattern when the Grashof number exceeds a critical value. This transition has been observed experimentally by Vest and Arpaci [5]. The critical Grashof number is weakly dependent on the Prandtl number, having the approximate value $Gr_c = 7700 \pm 5\%$. For a high Prandtl number fluid ($Pr > 12.7$), the unstable parallel flow becomes a pair of oscillatory travelling waves moving in opposite directions, and the critical Grashof number decreases as the Prandtl number increases. Korpela *et al.* [3] and Choi and Korpela [6], based on the results of Hart [7], concluded that the instability of the basic flow for a small Prandtl number fluid is induced by the shear mode, while for a high Prandtl number fluid, instability is caused by the buoyant mode.

It is well known that the stability of a flow driven by combined shear and buoyancy forces is relevant to many industrial processes (such as heat pipe, and reactor core). These problems have not received adequate attention in the past. Recently, Mohamad and Viskanta [8] considered the effect of a shear stress resulting from the motion of the upper lid on the stability properties of the Rayleigh–Bénard problem. Their results showed that the flow is stabilized by the presence of a shear force for the values of the parameters they investigated ($Pr = 0.01$ and 1). They also found that the travelling wave is generated by a moving lid.

In the present study, we consider the linear stability of natural convection in a tall vertical slot while accounting for the influence of a shear force induced by the motion of the sidewall. In this problem, the basic flow is the Poiseuille flow, a buoyancy-driven flow, superposed by the Couette flow, a forced flow. It is well known that the Couette flow is always stable. Therefore, it is of interest to investigate the effect of a shear force on natural convection stability in a tall vertical slot. We chose the Reynolds, Grashof, and Prandtl numbers as the externally controllable parameters necessary to characterize the problem at hand. The effect of the Reynolds and Prandtl numbers on the critical Grashof number, critical wave number, and critical wave speed has been investigated.

2. FORMULATION

Consider two infinitely long, vertical parallel plates of distance L enclosing a Newtonian fluid. The temperatures of the left and right plates are T_1 and T_2, respectively. The right plate is moving up at a constant velocity U_p. Figure 1 shows the problem configuration. The temperature difference is assumed to be small enough so that the density is treated as a constant everywhere in the governing equation, except in the gravitational term. The kinematic viscosity ν, thermal diffusivity α, and thermal expansion coefficient β are assumed to be constant.

We seek a steady, parallel flow solution for the form $(u, v, w, p, \theta) = [U(y), 0, 0, P(y), \Theta(y)]$. Assuming this to be possible, the solution for the basic state is given by

$$U = -Re(2y-3y^2)/Gr-(y-3y^2+2y^3) \quad (1)$$

$$\Theta = y-1/2 \quad (2)$$

where $Re = U_pL/\nu$ is the Reynolds number and $Gr = g\beta\Delta TL^3/\nu^2$ the Grashof number. In equations (1) and (2), all quantities have been non-

NOMENCLATURE

g	acceleration of gravity
Gr	Grashof number
Gr_c	critical Grashof number
k	wave number in the x-direction
m	wave number in the z-direction
L	spacing between plates
p	dimensionless pressure
P	dimensionless pressure of basic state
Pr	Prandtl number
Re	Reynolds number
RG	ratio of Re to Gr
t	dimensionless time
T_m	mean temperature of sidewalls
ΔT	temperature difference between the sidewalls
u, v, w	x, y, z-dimensionless velocity components
U	dimensionless velocity of the basic state
U_p	velocity of the moving right sidewall
U_s	basic velocity at the inflection point
x	dimensionless, vertical coordinate opposite to gravity
y	dimensionless, horizontal coordinate normal to wall.

Greek symbols

α	thermal diffusivity
β	thermal expansion coefficient
θ	dimensionless temperature
Θ	dimensionless temperature of basic state
ν	kinematic viscosity
ρ	density
σ	complex growth rate.

Superscript

$'$	perturbation quantity.

dimensionalized using the scales L, L^2/ν, and $g\beta\Delta TL^2/\nu$ for length, time, and velocity, respectively. The dimensionless temperature is defined as $[T-T_m]/\Delta T$.

We applied infinitesimal disturbances to the governing equations using a standard method as follows:

$$(u, v, w, p, \theta) = (U, 0, 0, P, \Theta)+(u', v', w', p', \theta'). \quad (3)$$

After substitution into the governing equations and boundary conditions, we eliminated the portion resulting solely from the basic state, ignored second- and higher-order terms, and assumed normal modes

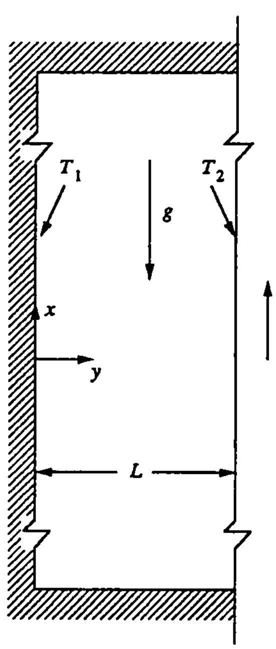

Fig. 1. Schematic diagram of the physical system.

of the form:

$$(u', v', w', p', q') = [u^*(y), v^*(y), w^*(y), p^*(y), \theta^*(y)] \times \exp(\mathrm{i}kx+\mathrm{i}mz-\mathrm{i}\sigma t) \quad (4)$$

where k and m are disturbance wave numbers in the x and z directions, respectively. The complex eigenvalue σ

$$\sigma = \sigma_r+\mathrm{i}\sigma_i \quad (5)$$

contains the growth rate σ_i and the frequency σ_r. If $\sigma_i > 0$ the basic state is unstable, while if $\sigma_i < 0$, it is linearly stable.

The linear disturbance equations become

$$\mathrm{i}ku^*+\mathrm{D}v^*+\mathrm{i}mw^* = 0 \quad (6a)$$

$$-\mathrm{i}\sigma u^*+\mathrm{i}k\,Gr\,Uu^*+Gr(\mathrm{D}U)v^* = -\mathrm{i}k\,Gr\,p^*+\theta^*+(\mathrm{D}^2-m^2-k^2)u^* \quad (6b)$$

$$-\mathrm{i}\sigma v^*+\mathrm{i}k\,Gr\,Uv^* = -Gr\,\mathrm{D}p^*+(\mathrm{D}^2-m^2-k^2)v^* \quad (6c)$$

$$-\mathrm{i}\sigma w^*+\mathrm{i}k\,Gr\,Uw^* = -\mathrm{i}m\,Gr\,p^*+(\mathrm{D}^2-m^2-k^2)w^* \quad (6d)$$

$$Pr[-\mathrm{i}\sigma\theta^*+\mathrm{i}k\,Gr\,U\theta^*+Gr(\mathrm{D}\Theta)v^*] = (\mathrm{D}^2-m^2-k^2)\theta^* \quad (6e)$$

where $\mathrm{D} = \mathrm{d}/\mathrm{d}y$, and the Prandtl number is defined as $Pr = \alpha/\nu$. The boundary conditions remain

$$u^* = v^* = w^* = \theta^* = 0 \quad \text{at } y = 0 \text{ and } 1. \quad (7)$$

According to the Squire theorem [9], the critical Grashof number can be obtained by considering two dimensional disturbances. By selecting $m = w = 0$, the linear disturbance equations for the marginal state ($\sigma_i = 0$) are

$$iku^* + Dv^* = 0 \quad (8a)$$

$$-i\sigma_r u^* + ik\,Gr\,Uu^* + Gr(DU)v^* = -ik\,Gr\,p^* + \theta^* + (D^2 - k^2)u^* \quad (8b)$$

$$-i\sigma_r v^* + ik\,Gr\,Uv^* = -Gr\,Dp^* + (D^2 - k^2)v^* \quad (8c)$$

$$Pr[-i\sigma_r\theta^* + ik\,Gr\,U\theta^* + Gr(D\Theta)v^*] = (D^2 - k^2)\theta^* \quad (8d)$$

with

$$u^* = v^* = \theta^* = 0 \quad \text{at } y = 0 \text{ and } 1. \quad (9)$$

The disturbance equations (8) with boundary conditions (9) are solved numerically using a standard shooting procedure without orthonormalization. In this numerical procedure, a fourth-order Runge–Kutta scheme is used to integrate the disturbance equations. The number of integration steps employed in the calculations is 100. From these calculations and subsequent use of Newton's method, values of Gr and ω corresponding to marginal stability are obtained for fixed k, Re and Pr. For given values of Re and Pr, the critical Grashof number Gr_c is the smallest marginal value of Gr over the space of wave number k.

The computations described in this section were done in double-precision arithmetic on the National Central University Micro-Vax 3600 computer.

3. RESULTS AND DISCUSSION

The stability of natural convection in a vertical slot has been studied by Korpela *et al.* [3], using the Galerkin method to solve the linear disturbance equations. To justify our numerical results, test computations have been performed for $Re = 0$. The critical Prandtl number at the transition between the shear mode and buoyant mode predicted by the present code is 12.5, which is very close to the prediction in ref. [3] ($Pr = 12.7$). The critical Grashof numbers for different Prandtl numbers are within 1% of the values listed in Table 1 of ref. [3].

Figure 2 shows basic-state velocity profiles obtained from equation (1). The dimensionless parameter RG that appears in Fig. 2 represents the ratio of Re to Gr. If $RG > 0$, the sidewall is moving up. For $RG = 0$, the vertical flow is induced only by the buoyancy force and is antisymmetric along the center of the slot. When Re is not equal to zero, the basic flow is a combination of the forced and buoyancy-driven flows, and the distribution of the vertical velocity is no longer antisymmetric. Fjørtoft's theorem [9] states that a necessary condition for an inviscid parallel flow to be linearly unstable is that $\Phi = U''(U'' - U_s) < 0$ somewhere in the flow field, where U_s is the velocity at the inflection point. Figure 3 is a plot of Φ vs y for different RG. When $RG = 0$, $\Phi(y)$ is symmetric along $x = 0.5$, and its value is negative except at the center and slot boundaries. Based on Fjørtoft's theorem, it seems reasonable to infer that the two opposite travelling waves in the slot for $Re = 0$ and $Pr > 12.7$ are induced by the antisymmetric vertical velocity profile generated by the buoyancy force. In other words, two boundary layers moving in opposite directions cause two oscillatory travelling waves also moving in opposite directions. For convenience, we chose mode A to denote the instability generated by the shear force, mode B for the boundary layer near the left wall and mode C for the boundary layer near the right wall. Looking at Fig. 3 in light of Fjørtoft's theorem, it is clear that for $Re \neq 0$, mode B is more unstable than mode C.

Figures 4 and 5 are plots of Gr_c vs Pr for different values of Re. As expected, the stability boundary for $Re = 0$ determined by mode B coincides with the boundary based on mode C. We see from Fig. 4 that for $Re = -100$, mode A is least unstable for small Prandtl number fluids ($Pr < 8.1$). For $8.1 < Pr < 10$, the most unstable mode is C, and for further increases in Prandtl number, the most unstable mode is B. For $Re = -200$, the instability structure for $Pr < 9$ is mode A. As Pr increases, mode A is replaced by mode B, and mode C does not appear. Our conjecture is that the critical Prandtl number at the transition between

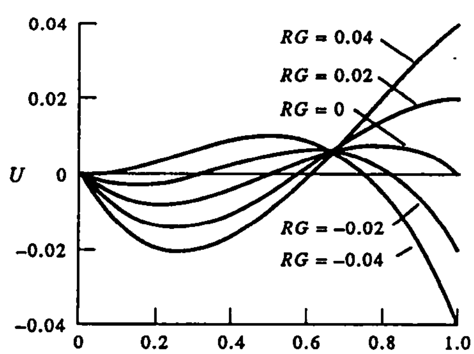

FIG. 2. Basic-state velocity profiles.

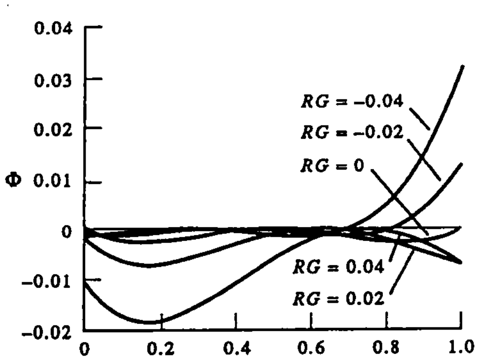

FIG. 3. Function Φ vs position y for different RG.

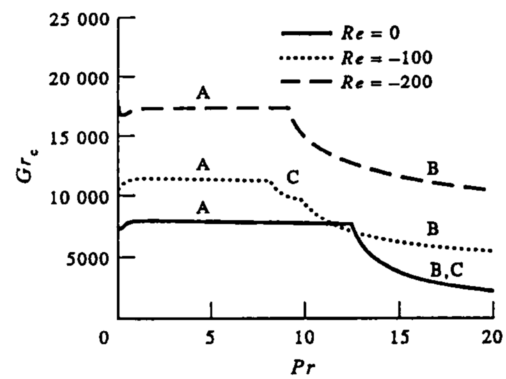

FIG. 4. The critical Grashof number vs Prandtl number for $Re = 0$, -100 and -200.

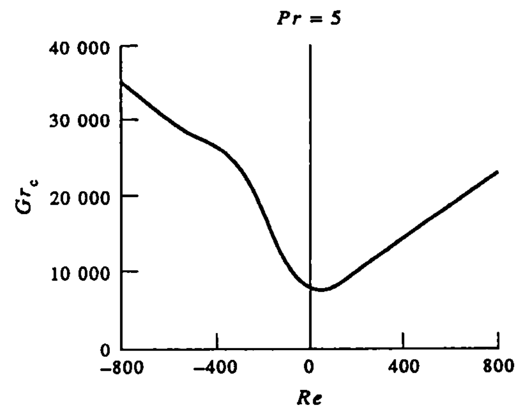

FIG. 6. The critical Grashof number vs Reynolds number for $Pr = 5.0$.

shear and buoyant modes decreases as Re increases when the effect of mode C is not taken into consideration. For $-150 < Re < 0$, the mode C induced by the buoyant force is most unstable in the area around $Pr = 10$, and if this effect is not taken into consideration, the predicted transition point will be higher than it is in actuality. Obviously, the critical Grashof number Gr_c increases with decreasing Re except for values of Pr near 10. In the region near $Pr = 10$, the flow may be destabilized because of a switch in the instability mode. When $Re > 0$, the critical Prandtl number at the transition between shear and buoyant modes increases as Re increases, and they are 15.6 and 19.5 for $Re = 50$ and 100, respectively. The buoyant instability is generated by mode B. Where mode B is dominant (higher Pr), the critical Grashof number Gr_c increases when Re increases. For smaller Pr ($Pr < 12.5$), the instability is induced by the shear mode (mode A), and the critical Grashof number Gr_c decreases with decreasing Re until the Reynolds number reaches a certain critical value: Re_c. For $Re > Re_c$, the critical Grashof number increases as Re increases. When $Re < 0$, Re_c does not appear and the flow continues to stabilize with increasing $|Re|$. The critical Reynolds number Re_c is weakly dependent on Pr, and its value is around $Re = 50$. Figure 6 is a typical example of the effect of variations of Re on Gr_c for small Prandtl number fluids.

Like the previous studies [6], the neutral curve for variations in wave numbers with Grashof numbers has two minima for $Re = 0$. The higher value of the wave number minimum defines the instability induced by the shear mode (mode A), while the lower values represent the instability induced by the buoyant modes (modes B and C). For small Prandtl numbers the shear force defines the instability, and the higher wave number of the two minima is the critical value. For $Re \neq 0$, two lower values of the wave number minimum appear and three minima are found. The wave number minimum caused by mode C is smaller than that induced by mode B. Figures 7 and 8 are plots of the critical wave number k_c vs Prandtl numbers for different Re. The discontinuous points represent the locations where the mode transition occurs. For

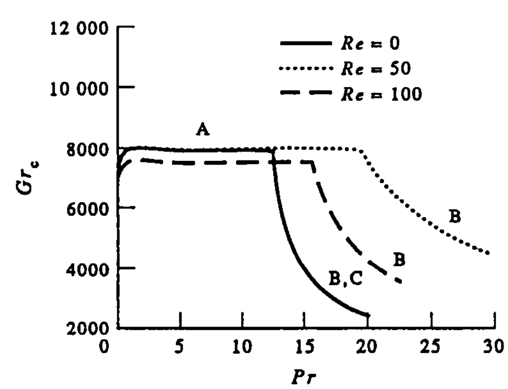

FIG. 5. The critical Grashof number vs Prandtl number for $Re = 0$, 50 and 100.

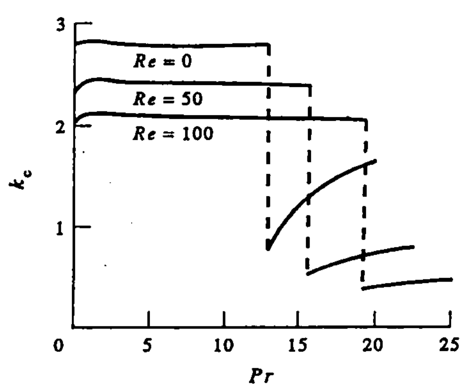

FIG. 7. The critical wave number vs Prandtl number for $Re = 0$, 50 and 100.

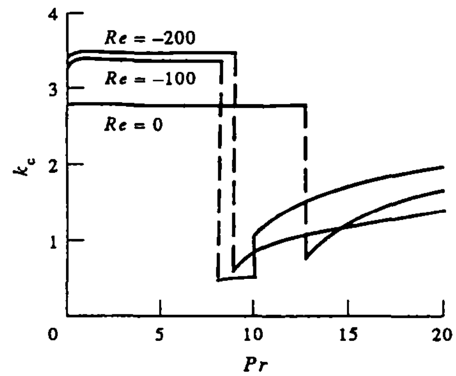

FIG. 8. The critical wave number vs Prandtl number for $Re = 0$, -100 and -200.

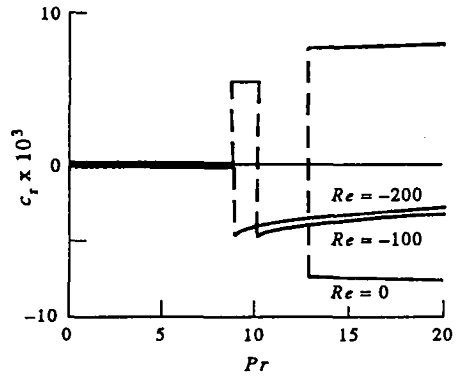

FIG. 10. The critical wave speed vs Prandtl number for $Re = 0$, -100 and -200.

smaller Pr, the critical wave number k_c is weakly dependent on Pr, while for higher Pr, it increases as Pr increases. The critical wave number is a strong function of Re. From Fig. 7, it is clear that for $Re > 0$ the wave number increases when Re increases. When the shear mode is dominant, the critical wave number increases with decreasing Re for $Re < 0$. For $Re = -100$ and $8.1 < Pr < 10$, the critical wave number is determined by mode C.

The critical wave speed is defined as $c_r = \sigma_r/(k_c Gr_c)$. Figures 9 and 10 demonstrate the critical wave speed variation of Pr for different Re. The critical wave speed is a very weak function of the Prandtl number, as the shear mode (mode A) dominates the instability. This is contrary to the case of $Re = 0$, in which the multicell flow pattern for $Re \neq 0$ is no longer stationary. The flow is driving upward ($c_r > 0$) for $Re = -200$, 50 and 100, while it is moving downward ($c_r < 0$) for $Re = -100$. As the Prandtl number increases above a certain value, the value of the critical wave speed switches to a higher value in which the buoyant mode is dominant. For $Re = 0$, two critical wave speeds having the same magnitude with different

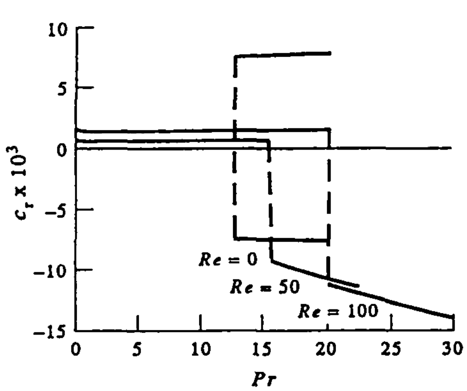

FIG. 9. The critical wave speed vs Prandtl number for $Re = 0$, 50 and 100.

sign appear at a fixed Pr as the buoyant force dominates the instability. Therefore, the unstable parallel flow becomes a pair of oscillatory travelling waves with the right boundary layer moving upward, induced by mode C, and the left boundary layer moving downward generated by mode B. For the Reynolds numbers considered here, downward travelling waves ($c_r < 0$) are predicted when the instability is dominated by the buoyant force, except for $Re = 100$ and $8.1 < Pr < 10$, where the travelling wave is moving upward ($c_r > 0$). When mode B is dominant, the travelling wave speed decreases as Re increases.

4. CONCLUSIONS

The linear stability of a flow field induced by the combination of a thermal buoyancy force and a shear force arising from a moving sidewall in a vertical slot has been studied. The results show three different kinds of instability: one shear mode and two buoyant modes. When the instability is dominated by the shear mode (for small Prandtl number fluids) the results show that the flow is stabilized by the downward motion of the right sidewall, which is initially destabilized by a very small upward velocity, and then restabilized for faster upward velocities. For instability states dominated by a buoyant mode generated by the left boundary layer (for high Prandtl number fluids), the flow is stabilized by either the upward or downward motion of the right sidewall. Three wave minima are found where the higher value corresponds to the instability generated by the shear mode and the smaller values to the buoyant instability. For a fluid with a Prandtl number near 10, the parallel flow may be destabilized by a small downward velocity of the sidewall since the most unstable mechanism is switched from a shear mode to a buoyant mode. The buoyant instability induced by the right boundary layer only appears for fluids with Prandtl numbers near 10 subjected to a slight downward motion of the sidewall. Based on our results and taking into account the effect of sidewall motion, the unstable flow in a tall slot will not become stationary no matter which mode is dominant.

Acknowledgements—This work is supported by the National Research Council of the R.O.C. under Grant No. NSC80-0401-E008-08.

REFERENCES

1. G. M. Gershuni, Stability of the pane convective motion of a liquid, *Zh. Tech. Fiz.* **23,** 1838–1844 (1953).
2. R. N. Rudakov, Spectrum of perturbations and stability of convective motion between vertical planes, *Prikl. Mat. Mekh.* **31,** 349–355 (1967).
3. S. A. Korpela, D. Gözüm and C. B. Baxi, On the stability of the conduction regime of natural convection in a vertical slot, *Int. J. Heat Mass Transfer* **16,** 1683–1690 (1973).
4. D. W. Ruth, On the transition to transverse rolls in an infinite vertical fluid layer—a power series solution, *Int. J. Heat Mass Transfer* **22,** 1199–1208 (1979).
5. C. M. Vest and V. S. Arpaci, Stability of natural convection in a vertical slot, *J. Fluid Mech.* **36,** 1–15 (1969).
6. I. G. Choi and S. A. Korpela, Stability of the conduction regime of natural convection in a tall vertical annulus, *J. Fluid Mech.* **99,** 725–738 (1980).
7. J. E. Hart, Stability of the flow in a differentially heated inclined box, *J. Fluid Mech.* **47,** 547–576 (1971).
8. A. A. Mohamad and R. Viskanta, Stability of lid-driven shallow cavity heated from below, *Int. J. Heat Mass Transfer* **32,** 2155–2166 (1989).
9. P. G. Drazin and W. H. Reid, *Hydrodynamic Stability*, p. 132. Cambridge University Press, Cambridge (1981).